NASA TECHNICAL MEMORANDUM

NASA TM X-53278

June 14, 1965

NASA TM X-53278

LIQUID CAVITATION STUDIES IN CIRCULAR PIPE BENDS

by R. E. STONEMETZ
Propulsion and Vehicle Engineering Laboratory

NASA

George C. Marshall
Space Flight Center,
Huntsville, Alabama

TECHNICAL MEMORANDUM X-53278

LIQUID CAVITATION STUDIES IN CIRCULAR PIPE BENDS

by

R. E. Stonemetz

George C. Marshall Space Flight Center
Huntsville, Alabama

ABSTRACT

Incipient cavitation indices were determined for various circular pipe bends using water as the working fluid. For all configurations investigated, the cavitation index decreased with increasing Reynolds Number and ratio of the fluid vapor pressure to the upstream dynamic pressure. The critical cavitation index was greater for smaller ratios of bend radii to pipe diameter; the angle of the bend had little effect. An empirical relationship was derived for the determination of the critical cavitation index. This relationship takes into account the effects of bend radius and pipe diameter.

NASA - GEORGE C. MARSHALL SPACE FLIGHT CENTER

NASA - GEORGE C. MARSHALL SPACE FLIGHT CENTER

TECHNICAL MEMORANDUM X-53278

LIQUID CAVITATION STUDIES IN CIRCULAR PIPE BENDS

By R. E. Stonemetz

PROPULSION AND VEHICLE ENGINEERING LABORATORY
RESEARCH AND DEVELOPMENT OPERATIONS

TABLE OF CONTENTS

LIST OF ILLUSTRATIONS

LIST OF TABLES

DEFINITION OF SYMBOLS

Symbol	Definition
d	pipe diameter
R	pipe bend radius
R/d	pipe bend radius ratio
$P_v/\frac{1}{2}\rho\overline{v}^2$	ratio of liquid vapor pressure to dynamic pressure
$\frac{\rho\overline{v}d}{\mu}$	Reynolds number
P_s	upstream static pressure
P_k	upstream static pressure at cavitation
$\overline{v}_k$	upstream mean velocity pressure at cavitation

LIQUID CAVITATION STUDIES IN CIRCULAR PIPE BENDS

SUMMARY

Incipient cavitation indices were determined for bends of 60°, 90°, and 120° in one plane for pipe diameters (d) of 1.5, 2.0, and 4.0 inches, and bend radius ratios (R/d) of 0.7, 1.0 and 1.5. The working fluid was water.

It was found that, for all configurations investigated, the critical cavitation index decreased somewhat with increasing values of Reynolds number and ratio of the fluid vapor pressure to the upstream dynamic pressure. The critical cavitation index was greater for smaller ratios of bend radius to pipe diameter. The bend angles investigated, 60° - 120°, had insignificant effect.

An empirical relationship was derived for the determination of the critical cavitation index. This relationship takes into account the effects of bend radius and pipe diameter.

INTRODUCTION

The phenomenon of cavitation in curved pipes is of importance to the Aerospace Industry, because short space vehicle stages require propellant suction ducts with small bend radii and large bend angles. These configurations are conducive to bend cavitation at the required high volume flowrates.

Much is available in the literature on cavitation concerning flow about bodies of various shapes, but little has been published on cavitation in pipe bends. The purpose of this investigation was to obtain experimental data on cavitation in pipe bends over a range of Reynolds numbers and ratios of vapor pressure to dynamic pressure (Pressure Ratio).

APPARATUS AND PROCEDURE

The bend configurations tested are shown in FIGURES 2 and 3. The bends were affixed to the side of a cylindrical sump at the bottom of a vertical cylindrical open top tank (reservoir) with a hemispherical shape bottom. FIGURE 1 shows the arrangement of the test tower. The overall height was 62 feet. The height from ground level to the test section was 39.75 feet. The flowrate was regulated by replaceable orifices near the bottom of the downcomer. The working fluid was water.

A three-probe static pressure pickup arrangement was used to measure the average upstream static pressure. Single measurements, directly opposite one another, were made in the bend (FIGURE 3). In all cases, the static pressure holes were polished to remove burrs. All pressures were recorded electrically.

The water reservoir was filled to a predetermined level and timed through a measured fall. The fall was of such magnitude that steady flow conditions were assumed to have been established (5 seconds) and that the pressure head differential could be neglected. In this way the volume flowrate was computed.

With a given orifice size and required tank liquid level, the shutoff valve was opened and a test was run. This procedure was repeated twice for each orifice size and for each test section; the orifice size was increased until cavitation was visually observed. Although more fully developed cavitation could be observed at slightly larger orifice sizes, a size was reached that produced no increase in flow velocity or volume flowrate.

For each run, maximum, minimum and mean values were determined for the pressure at each probe position. For each test the average of the maximum values of the pressure was chosen to be used in determining the cavitation indices because of the associated minimum data scatter. Flowrates also were determined from the average of two test runs per orifice size.

The water temperature ranged from 70° to 130°F in steps of approximately 15°F.

CAVITATION CRITERIA

The occurrence of cavitation in a curved pipe can be explained by examining the forces on an element of fluid as it passes through the bend. As the surface curves away from the element, an inward force must act on it to keep it against the inner surface. The outer wall pressure cannot increase; hence, the pressure difference required to keep the particle against the inner surface must be supplied by a reduction in the inner wall pressure. The maximum pressure difference is attained when the inner surface pressure has fallen to the vapor pressure of the liquid. However, if the outward radial velocity component of the particle has not fallen to zero, the pressure difference is not great enough to cause the particle to follow the path of the bend. Therefore, it separates from the inner wall and cavitation occurs (Ref. 1). This phenomenon is depicted by the test results shown in FIGURE 4.

Cavitating flows are described by the cavitation index or number:

$$\sigma = \frac{P_s - P_v}{\frac{1}{2}\rho \bar{v}^2} \tag{1}$$

where P_s is the upstream static pressure, P_v the vapor pressure at the bulk liquid temperature, ρ the mass density, and $\bar{v}$ the upstream mean velocity. The critical cavitation index, σ_k, is defined by:

$$\sigma_k = \frac{P_k - P_v}{\frac{1}{2}\rho \bar{v}_k^2} \tag{2}$$

The upstream static pressure at cavitation is P_k, the mean critical velocity at which cavitation occurs is $\bar{v}_k$, and P_v and ρ as before.

CAVITATION SIMILARITY LAWS

The similarity laws for curved pipe flow can be explained in the same manner as those for flow about a body. At some point within a pipe bend, a maximum flow velocity is reached with a corresponding minimum pressure. A minimum pressure coefficient is defined as:

$$c_{p_{min}} = \frac{P_s - P_{min}}{\frac{1}{2}\rho \bar{v}^2} \tag{3}$$

At the point of cavitation inception, for geometrically similar flow systems, the ratio of the pressure difference $P_s - P_{min}$ to the upstream dynamic pressure is equal to the minimum pressure coefficient in the non-cavitating flow regime (Ref. 2). Therefore, the assumption that the minimum pressure equals the vapor pressure and that the minimum pressure coefficient equals the critical cavitation index at cavitation inception makes equation 3 identical to equation 2.

The scaling laws (similarity laws) employed in this study are briefly outlined below:

(1) Maintain a constant ratio between the inertial and viscous fluid forces - Reynolds number.

$$R = \frac{\rho V d}{\mu} \tag{4}$$

(2) Assuming a near gas-free liquid, maintain a constant ratio of the vapor pressure to the dynamic pressure.

$$\frac{P_v}{\frac{1}{2}\rho V^2} \tag{5}$$

This scaling law can be used when all evaluations are made after cavitation inception. However, P_v will not necessarily be the vapor pressure at the bulk liquid temperature, because the vaporization of the liquid produces a cooling effect that lowers the vapor pressure. This reduction will be given by (Ref. 3)

$$\Delta P_v = \frac{\partial P_v}{\partial T} \Delta T \tag{6}$$

Hence, the scaling relationship should be $\Delta P_v / \frac{1}{2}\rho V^2$. In this study the evaluation of the critical cavitation index was not always made at the same point within the cavitation region during every test; consequently, some tests produced significant cooling effects and others almost none. Due to this inconsistency, P_v was taken to be the vapor pressure at the bulk liquid temperature and equation 5 to be the scaling relationship.

Actually, there are other parameters that could cause departures from the scaling laws. No consideration was given to the effect of dissolved air and/or gas within the liquid, or to the effect of the surface tension of the liquid. Also disregarded are the time effects of bubble growth by diffusion associated with gaseous type cavitation, such as that presented by Ref. 3. No attempt was made to control the surface roughness or to vary fluid cleanliness to account for variations in the availability of bubble nucleation sites (Ref. 4). Unfortunately, it is impossible to isolate one scaling parameter and study its effects on cavitation.

RESULTS AND DISCUSSION

The scaling relationships employed in this study were the Reynolds number and the pressure ratio. The Reynolds number was used to show how viscous effects alter the critical cavitation index. The experimental test arrangement (Figure 1) could not control pressure nor flow velocity; hence the point of cavitation inception could not be determined with accuracy. Therefore, all evaluations were made after cavitation inception, that is, within the "cavitation region." Wislicenus (Ref. 3) suggested using the pressure ratio as a scaling parameter because of the effects on the vapor pressure within the "region" caused by liquid vaporization.

Cavitation Region

The "cavitation region" is illustrated in FIGURE 5. It can be described as the region between the point of cavitation inception and the point where choked flow or steady state conditions prevail. The diagram shows that as the bulk liquid temperature rises ($T_5 > T_1$), the flow velocity decreases for incipient cavitation. Essentially, the liquid vapor pressure rises with temperature, thereby necessitating a lower mean flow velocity to induce cavitation. In turn, assuming frictionless flow, the upstream static pressure increases at the expense of a decrease in upstream velocity pressure. Table II is a compilation of experimental flow parameters and critical cavitation indices for various liquid temperatures, pipe bend angles, pipe bend radii, and pipe diameters. The table shows that the critical velocity for cavitation decreases as the liquid temperature increases for all configurations tested.

The "cavitation region" can best be explained by citing an example from the diagram (Figure 5). Assume incipient cavitation at an orifice diameter of 2.95 inches and a bulk liquid temperature of T_1. It can be visually observed that slightly more voluminous boiling occurs as the orifice diameter is increased in increments of 0.01 inch up to a diameter of 3.0 inches, all other conditions remaining unchanged. Any further increase in orifice diameter will produce no further increase in the amount of cavitation, and this point is the beginning of the choked flow region. In between is the "cavitation region."

Velocity Profile in Bend

Figure 2 depicts the experimental test section configurations. The 4-inch diameter test sections have a sharp-edged entrance at the sump that may be conducive to non-uniform velocity profiles. However, in all tests, cavitation occurred at the middle of the inside wall a short distance into the bend. This indicates that the velocity distribution was very uniform. Figure 3 shows a small amount of cavitation occurring on the inner surface of the 120° bend, 1.5 bend radius ratio, 2-inch diameter line. The exact origin of cavitation cannot be seen in the photograph because of a band of concentrated light reflecting from the periphery of the circular line within the plexiglass section; however, the photograph shows the pulsating effect associated with cavitation.

Discussion of Experimental σ_k

Experimental data shows that the upstream static pressure difference from one liquid temperature to another is small and is less than the vapor pressure difference over the same temperature range. Therefore, the magnitude of the numerator in equation 2 decreases with each temperature increment. Since the upstream dynamic pressure is a function of the upstream static pressure (assuming negligible friction pressure differential losses), its change will likewise be small. Therefore, the magnitude of the dynamic pressure decreases only slightly for each temperature increment, and less severely than the magnitude of the pressure difference in the numerator of equation 2. It can be concluded that the critical cavitation index decreases as the liquid temperature increases (Figures 6 and 7).

Several cavitation indices were found at the cavitation inception point for the 90^{o} bend, 1.0 bend radius ratio, 2-inch diameter line, and are depicted as curve (1) in Figures 6 and 7. These indices are approximately 25% higher than those found for the more voluminous visual cavitation. It should not be concluded, however, that the other test sections can be represented likewise, because such points for these test sections were not observed. This points to the fact that precise control of the pressure and flow velocity are of utmost importance for visual investigations of incipient cavitation phenomena.

Figures 6 and 7 reveal that the critical cavitation index is not solely a function of the Reynolds number nor the pressure ratio, but is affected by the line size and bend radius ratio. Hence, it appears that these terms should be included in the derivation or evaluation of the critical cavitation indices for curved pipe flow.

Let equation 2 be the defining equation for the critical cavitation index for straight pipe flow, and call equation 7 the defining equation for curved pipe flow.

$$\sigma k_c = \frac{P_k - P_v}{\frac{1}{2} v_k^2} - 0.67 \, (R/d)^{-d} \qquad (7)$$

The R/d for straight pipe flow is infinite and, when applied to equation 7, gives the defining equation for straight pipe flow (equation 2). Table I gives the values of the parameters for the second term of equation 7 as applicable to the test sections used in this investigation.

Table I. Values of R/d and $0.67 \, (R/d)^{-d}$ for Different Pipe Sizes and Bend Radius Ratios

R/d	d	$(R/d)^{-d}$	$0.67 \, (R/d)^{-d}$
∞	any size	0	0
1	2	1	0.67
1.5	2	0.445	0.30
1.5	4	0.20	0.13
4	2	0.0625	0.042

The predominant factor in the second term of equation 7 is the bend radius. For R/d values approaching 10, equation 7 approaches equation 2. Essentially, equation 7 combines the three distinct bands of Figure 7 into one band when plotted as a function of Reynolds number (Figure 8). This is desirable and appears to diminish the importance of the previously mentioned scale effects.

CONCLUSIONS

For a Reynolds number range of 4×10^5 to 2×10^6 and for a range of pressure ratios of 0.04 to 0.40, the following conclusions are made:

1. Cavitation occurring in pipes curved in one plane was found to be affected by the pipe bend radii and the pipe diameters, and affected little, if any, by the pipe bend angle.

2. In curved pipes, critical cavitation indices decrease in magnitude for increasing Reynolds number and pressure ratio $\frac{P_v}{\frac{1}{2}\rho V^2}$.

3. The empirical defining equation for the critical cavitation index of curved pipe flow (equation 7) in conjunction with Reynolds number appears to be an adequate scaling relationship.

4. Increasing the temperature of a liquid lowers its critical velocity for cavitation.

RECOMMENDATIONS

This study was conducted using the classical approach to the problem. Figure 8 reveals that there is some spreading of points which could be due to nuclei, gas or air content, etc., as well as to data scatter. Further studies should be conducted to determine just how important the aforementioned effects are on curved pipe-flow cavitation. A closed loop facility, having the capability of controlling either the pressure or velocity, or both, should be employed. In this way accurate cavitation inception indices may be determined for various bend configurations; lower and higher ranges of Reynolds numbers can be explored as well as the nuclei in the working fluid, air content, and upstream and downstream velocity profiles. A very important and rather simple investigation would be to determine whether critical cavitation indices at cavitation inception are repeatable for curved pipe flow.

Table II Critical Cavitation Indices and Related Parameters

90^{o} Bend, R/d = 1.0, 2 inch diam line

Orifice Diam (inc.)	Flow Velocity (ft/sec)	Water Temp (^{o}F)	Vel. Press. (PSF)	Vapor Press. (psia)	Re	P_k (psia)	$\frac{P_v}{\frac{1}{2}\bar{v}_k^2}$	k	kc
2.372	29.9	73	864	0.402	4.89×10^5	10.75	.067	1.72	1.05
2.372	30.1	81	873	0.530	5.44	10.81	.087	1.70	1.03
2.372	30.4	82	891	0.541	5.58	10.96	.087	1.68	1.01
2.372	29.8	110	852	1.275	7.32	11.00	.215	1.65	.98
2.372	29.2	128	815	2.106	8.59	11.10	.372	1.59	.92
			60^{o} Bend, R/d = 1.5, 2 inch diam line						
2.372	33.9	71	1114	0.376	5.38×10^5	9.91	.0486	1.23	.93
2.372	33.8	82	1100	0.541	6.24	9.35	.0708	1.15	.85
2.372	33.4	100	1075	0.935	7.44	9.52	.125	1.15	.85
2.372	32.8	112	1036	1.35	8.32	9.75	.188	1.17	.87
2.372	31.9	127	975	2.05	9.29	10.07	.307	1.19	.89
			90^{o} Bend						
2.650	33.4	66	1075	0.316	4.98×10^5	9.54	.0423	1.24	.94
2.650	33.3	82	1071	.514	6.11	9.49	.0728	1.20	.90
2.650	33.0	95	1052	.815	7.03	9.38	.116	1.17	.87
2.650	32.6	108	1018	1.203	7.92	9.57	.170	1.18	.88
2.650	31.2	124	930	1.890	8.82	9.88	.292	1.24	.94

Table II Continued

Orifice Diam (in.)	Flow Velocity (ft/sec)	Water Temp (^{o}F)	Vel. Press. (PSF)	Vapor Press. (psia)	Re	P_k (psia)	$\frac{P_v}{\frac{1}{2}\bar{v}_k^2}$	k	kc
		120^{o} Bend							
2.650	33.8	71	1103	0.369	5.34×10^5	9.75	0.0482	1.22	.92
2.650	33.5	82	1079	0.539	6.19	9.79	.0719	1.23	.93
2.650	32.9	94	1042	0.791	6.99	9.90	.109	1.26	.96
2.650	31.6	113	962	1.390	8.07	10.50	.208	1.36	1.06
		60^{o} Bend, R/d - 1.5, 4 inch diam line							
4.525	34.7	71	1165	0.376	1.11×10^6	7.94	.0465	0.94	.81
4.525	33.8	81	1104	0.517	1.22	7.52	.0674	.91	.78
4.525	34.9	98	1176	0.894	1.53	8.02	.109	.87	.74
4.525	33.9	114	1105	1.430	1.75	8.08	.186	.87	.74
4.525	33.2	127	1060	2.050	1.93	8.31	.278	.85	.72
		90^{o} Bend							
4.525	34.8	70	1172	0.363	1.10×10^6	8.43	0.0446	0.99	.86
4.525	33.3	81	1073	0.525	1.21	8.02	.0705	1.00	.87
4.525	34.2	85	1130	0.596	1.30	8.52	.0759	1.00	.87
4.525	33.9	105	1104	1.102	1.60	8.61	.144	.98	.85
4.525	33.5	129	1072	2.164	1.98	8.72	.291	.88	.75
		120^{o} Bend							
4.525	34.6	72	1160	0.389	1.12×10^6	8.10	0.0483	0.96	.83
4.525	34.7	79	1173	0.494	1.23	7.29	.0598	.84	.71
4.525	34.3	96	1132	0.841	1.47	8.14	.107	.93	.80
4.525	34.0	115	1113	1.471	1.78	8.40	.190	.90	.77
4.525	33.1	128	1052	2.106	1.95	8.73	.295	.91	.78

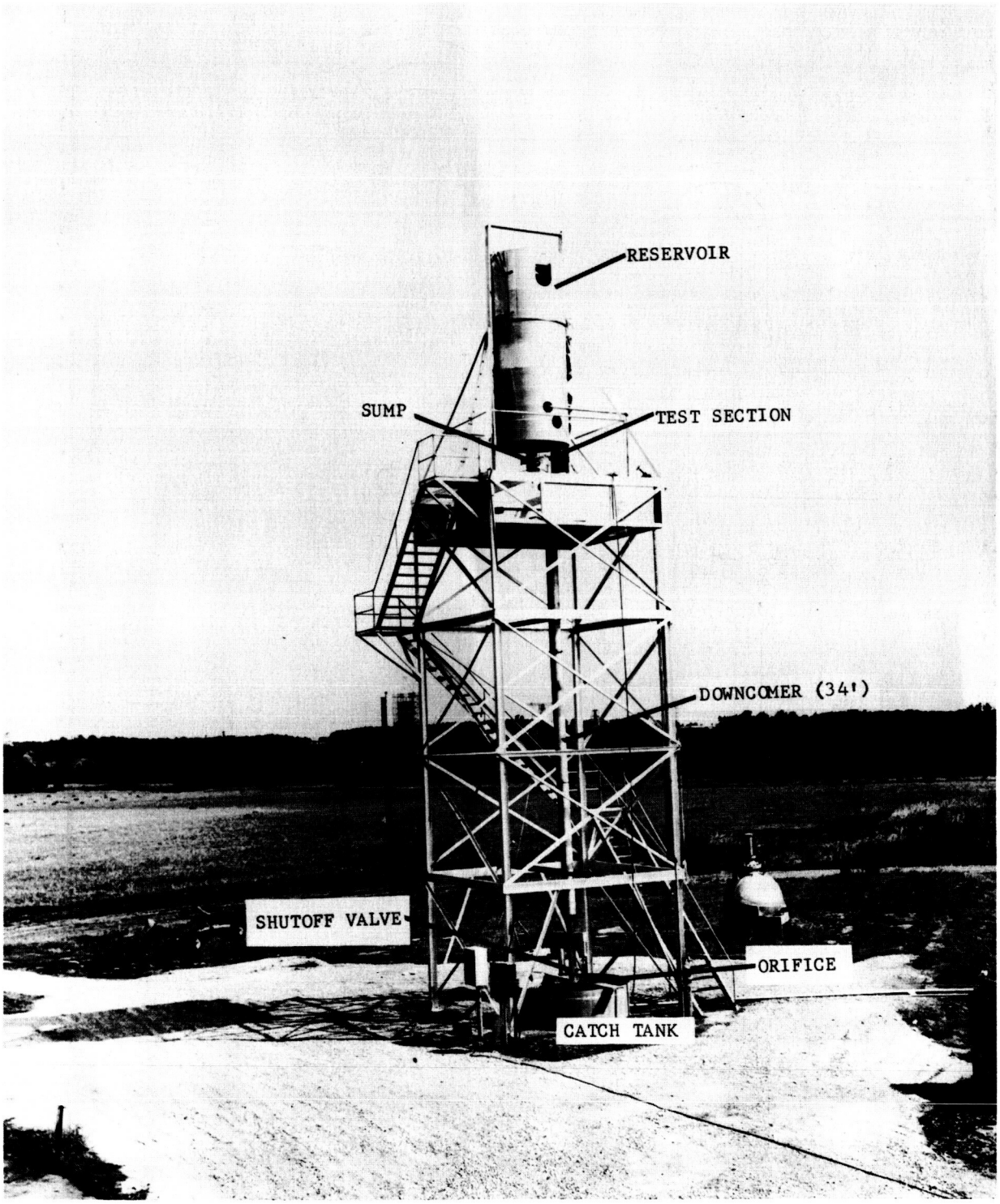

FIGURE 1. CAVITATION STUDY TEST ARRANGEMENT

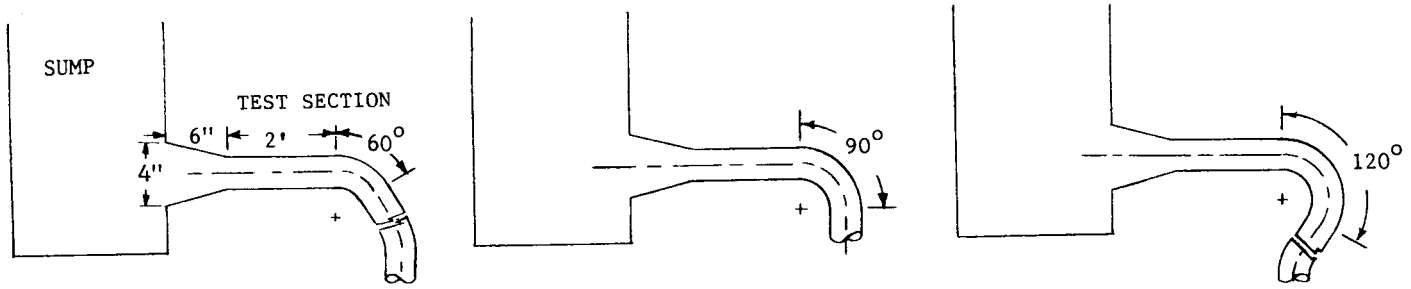

(a)

Test section bend angles of 60°, 90°, 120° for a 2 inch dia. line and an R/d = 1.5

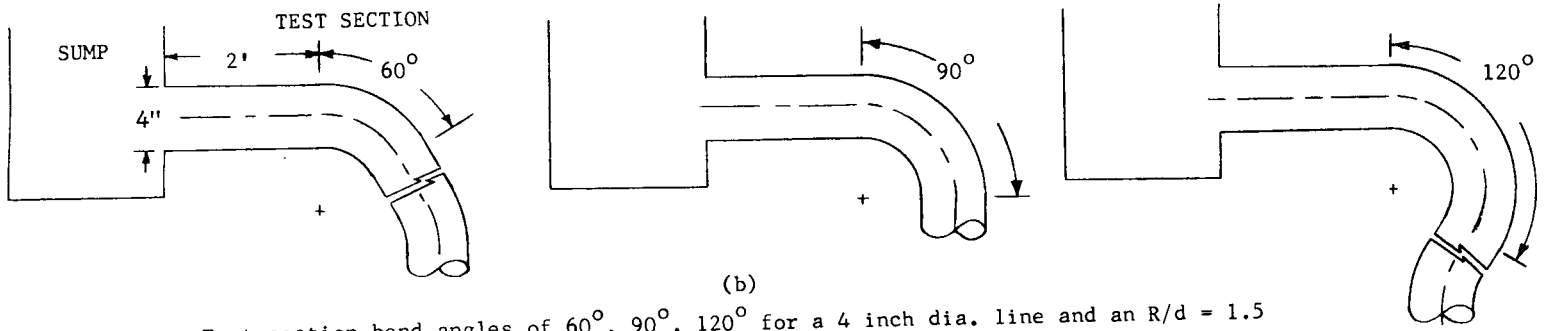

(b)

Test section bend angles of 60°, 90°, 120° for a 4 inch dia. line and an R/d = 1.5

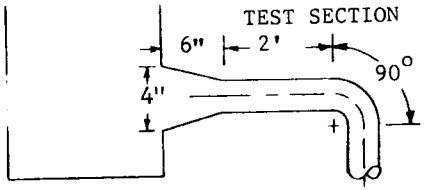

(c) 90° bend, 2 inch dia. line, R/d = 1.0

FIGURE 2. TEST SECTION CONFIGURATIONS

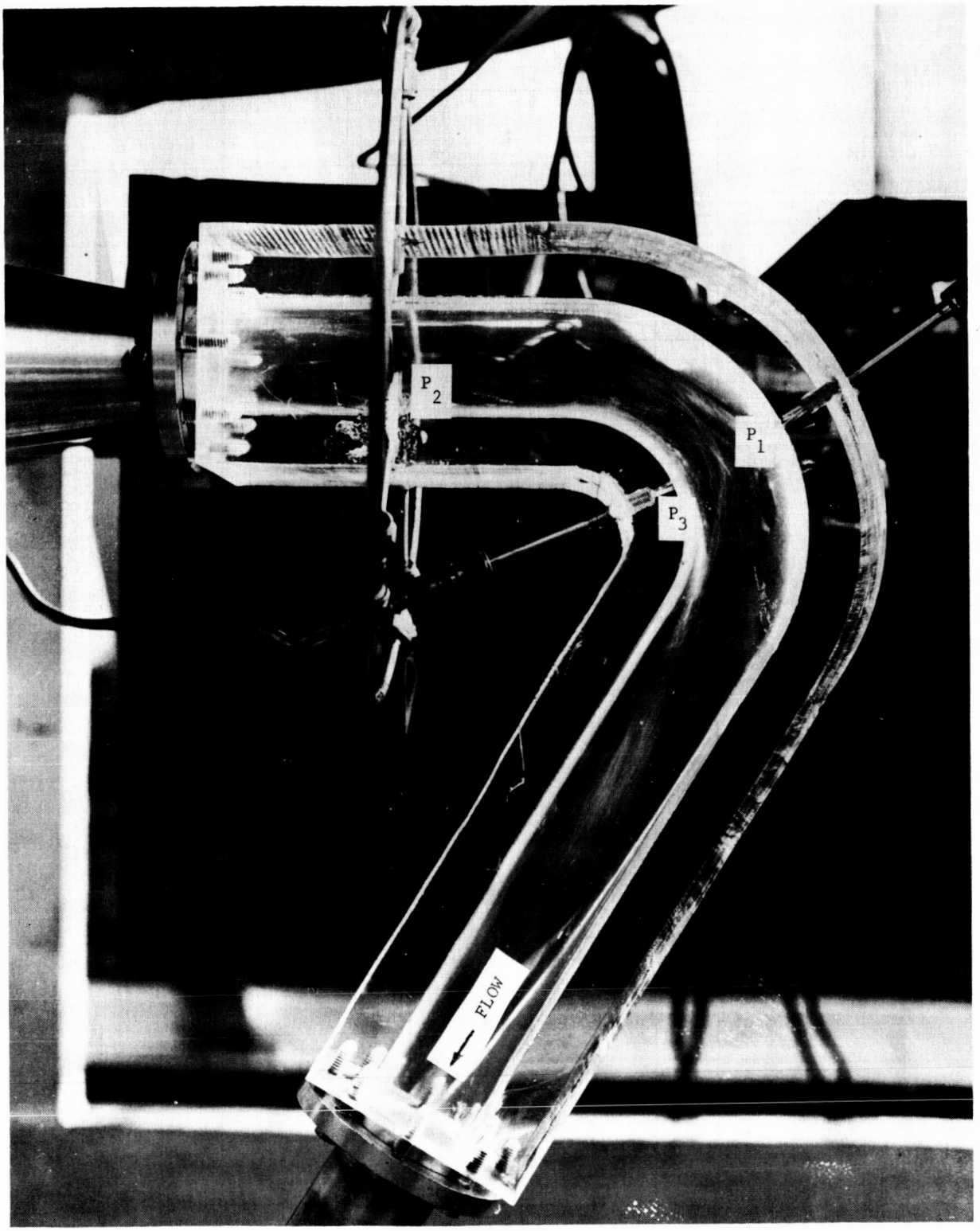

FIGURE 3. 120° BEND TEST SECTION SHOWING PROBE POSITIONS AND PULSATING CAVITATION (Shutter speed: 1/500th sec.)

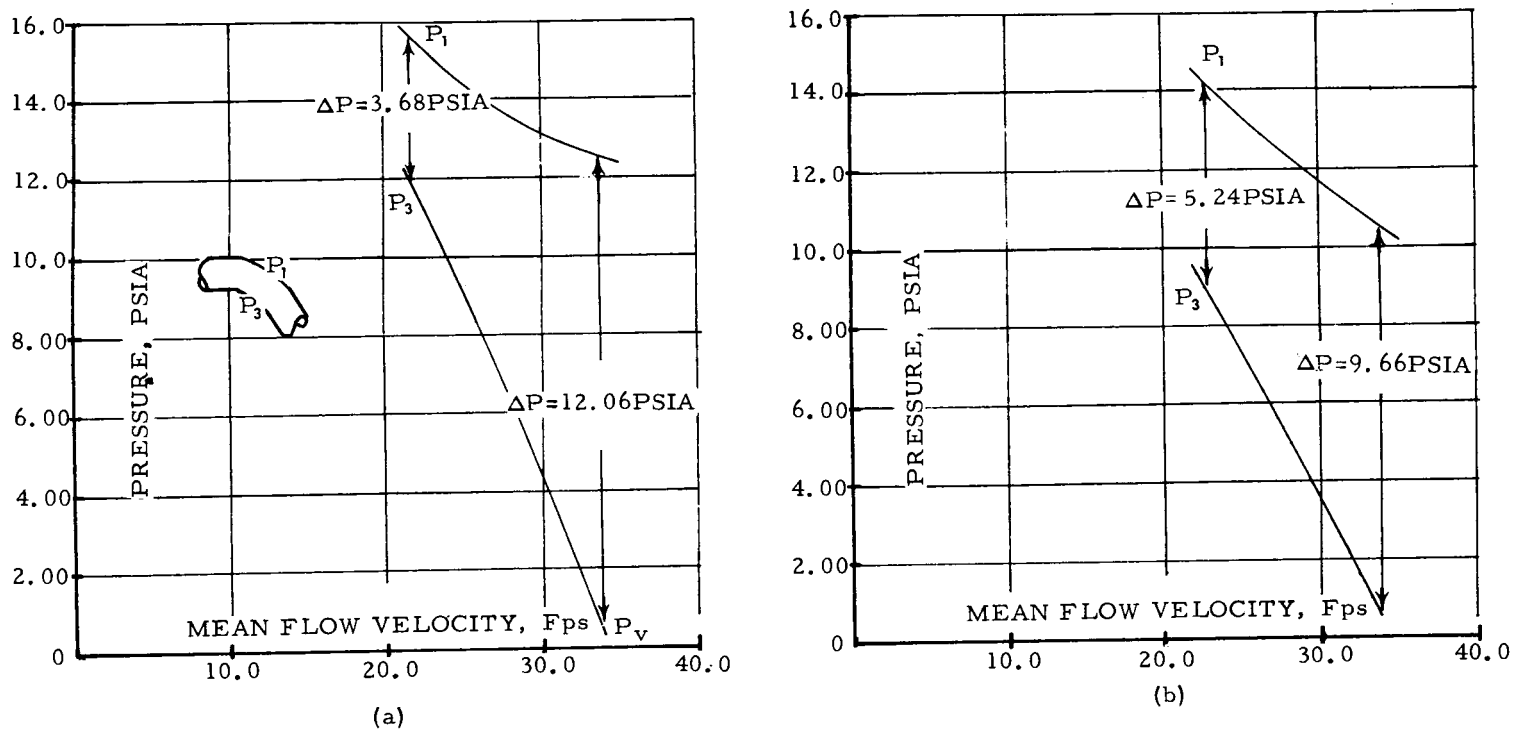

FIG 4. RADIAL PRESSURE DIFFERENTIALS ACROSS THE (a) 60° BEND, 2 INCH DIAM TEST SECTION AND THE (b) 60° BEND, 4 INCH DIAM TEST SECTION AT VELOCITIES UP TO THE MEAN CRITICAL FLOW VELOCITY AT A BULK WATER TEMPERATURE OF 80°F

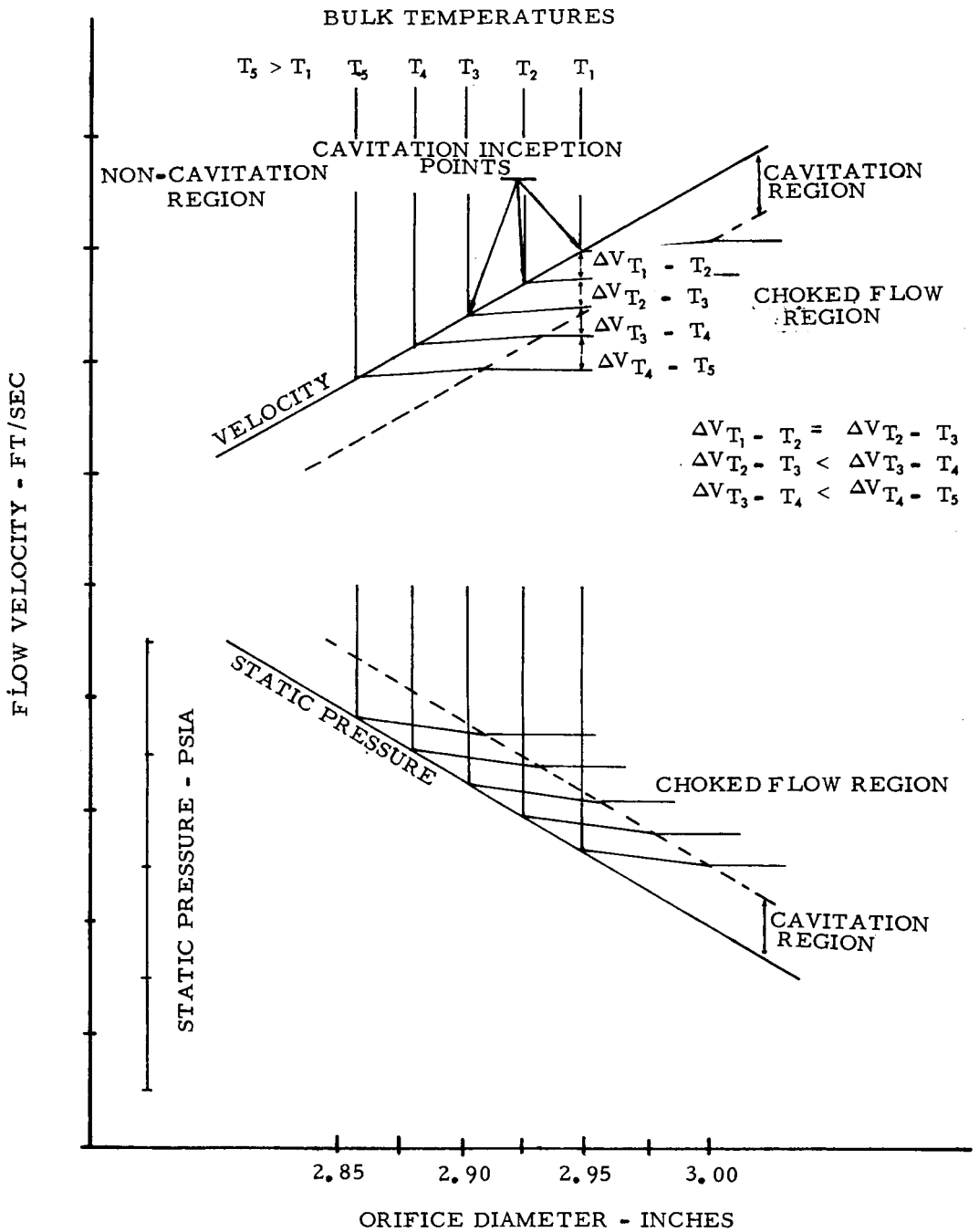

FIG 5. DIAGRAM OF REGIONS ENCOUNTERED IN CURVED PIPE FLOW AND THEIR EFFECTS ON THE CAVITATION PARAMETERS

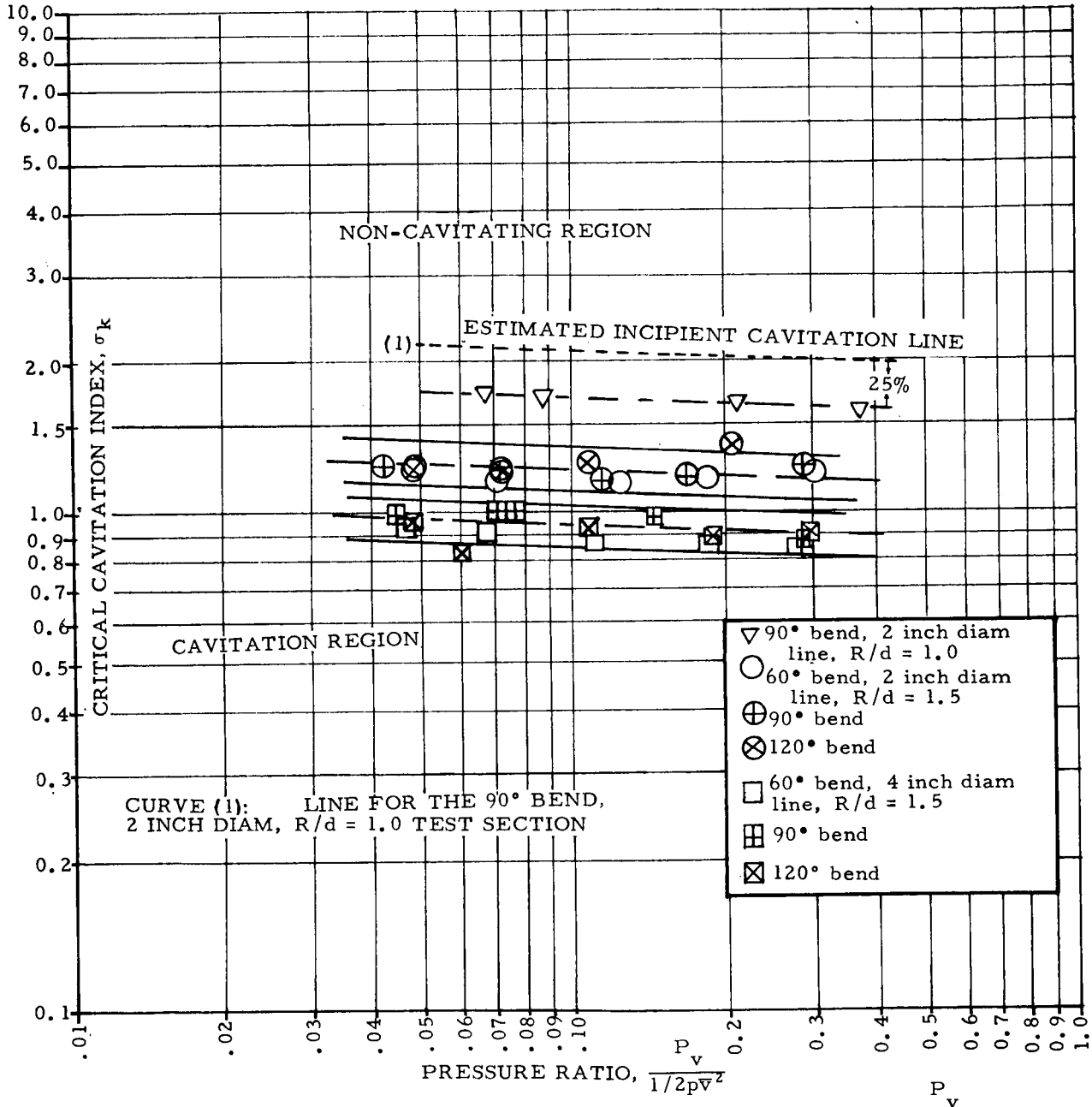

FIG 6. CRITICAL CAVITATION INDEX VS PRESSURE RATIO, $\frac{P_v}{1/2\rho\bar{v}_k^2}$, WITHIN THE CAVITATION REGION

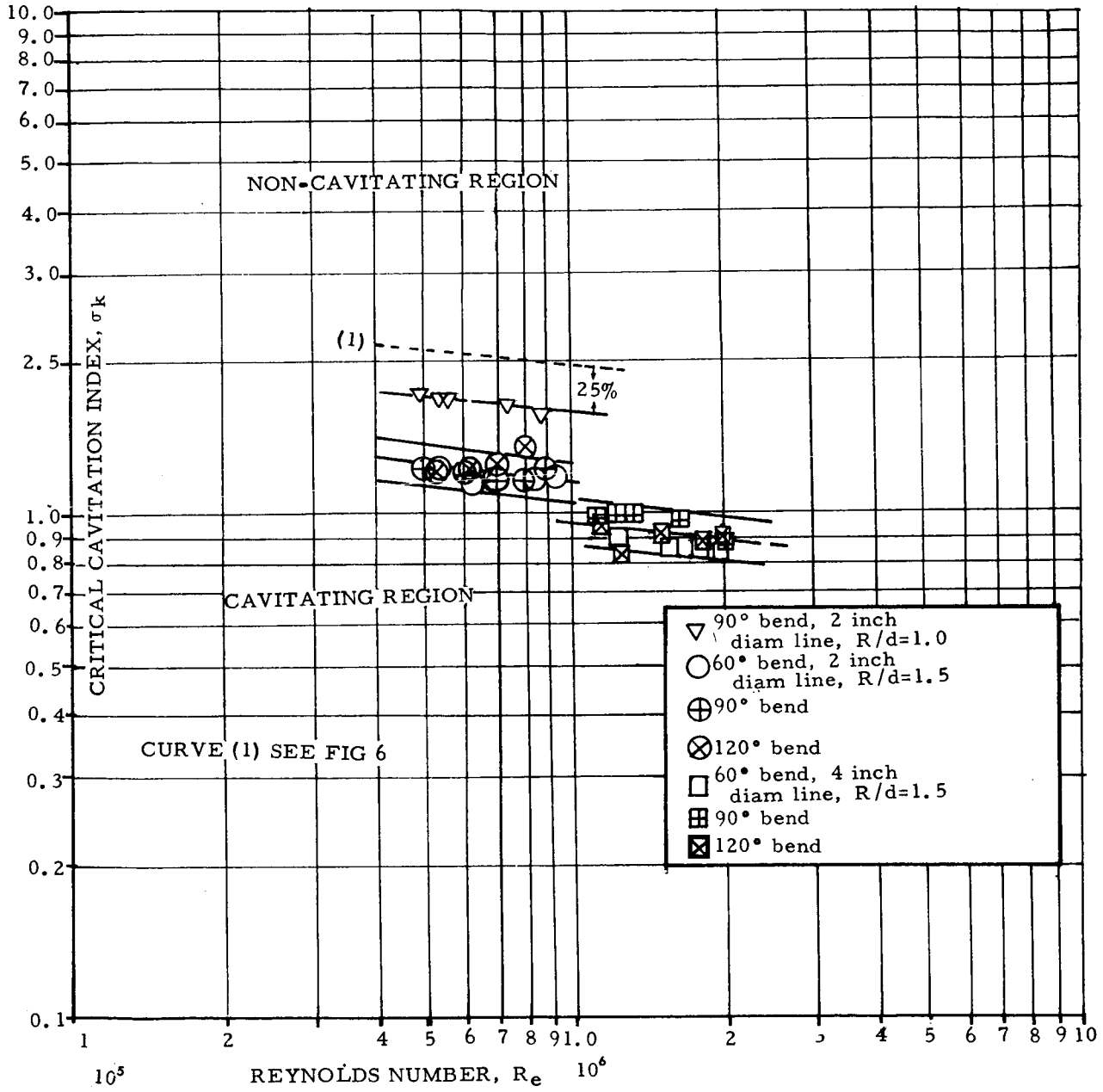

FIG 7. CRITICAL CAVITATION INDEX VS REYNOLDS NUMBER WITHIN THE CAVITATION REGION.

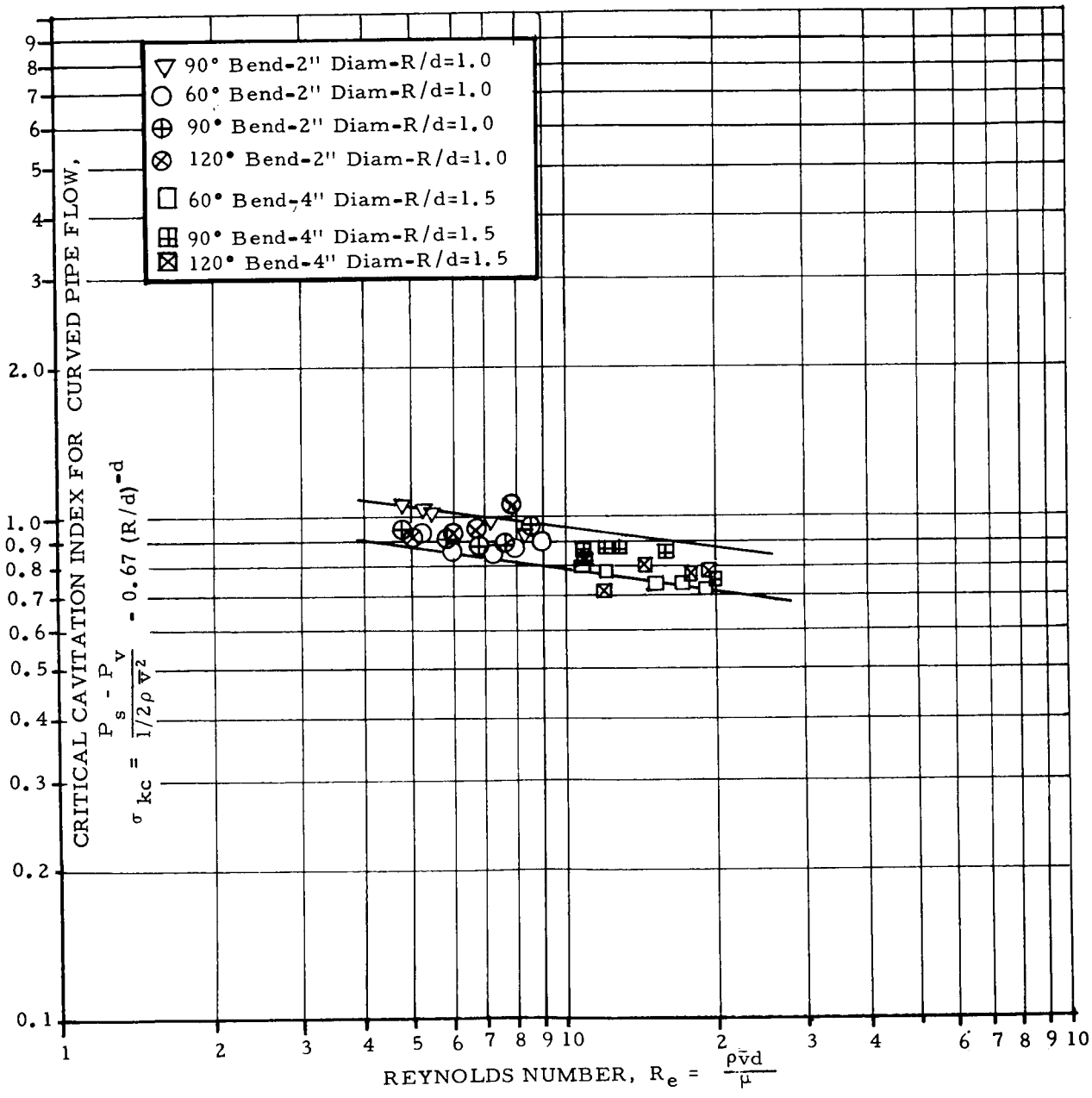

FIG 8. CURVED PIPE CRITICAL CAVITATION INDEX

AS COMPUTED VS REYNOLDS NUMBER

REFERENCES

1. Knapp, R. T., and A. Hollander, Laboratory Investigations of the Mechanisms of Cavitation, Trans ASME, July, 1948, pp. 419-435.

2. Hall, John William, The Effect of Surface Irregularities on Incipient Cavitation, Doctoral Thesis, The Pennsylvania State University, College Park, Pa., June, 1958, pp 11-14.

3. Hall, J. W., and George F. Wislicenus, Scale Effects on Cavitation, Trans. ASME, September, 1963, pp. 385-398

4. Harvey, E. N., McElroy, W. D., and A. H. Whitely, On Cavity Formation in Water, Journal of Applied Physics, Vol. 18, 1947, pp. 162-172.

LIQUID CAVITATION STUDIES IN CIRCULAR PIPE BENDS

By R. E. Stonemetz

The information in this report has been reviewed for security classification. Review of any information concerning Department of Defense or Atomic Energy Commission programs has been made by the MSFC Security Classification Officer. This report, in its entirety, has been determined to be unclassified.

This document has also been reviewed and approved for technical accuracy.

C. C. WOOD
Chief, Thermodynamics and Fluid Mechanics Branch

H. G. PAUL
Chief, Propulsion Division

for F. B. CLINE
Acting Director, Propulsion and Vehicle Engineering Laboratory

DISTRIBUTION

DIR		Dr. Von Braun
DEP-T		Dr. Rees
ASR-S		Dr. Lange
I-DIR		General O'Connor
I-SE-CH		Dr. Mrazek
V		Dr. Gruene
R-DIR		Mr. Weidner
R-FP-DIR		Dr. Koelle
R-RP-DIR		Dr. Stuhlinger
R-AERO-DIR		Dr. Geissler
R-ASTR-DIR		Dr. Haeussermann
R-COMP-DIR		Dr. Hoelzer
R-ME-DIR		Mr. Kuers
R-QUAL-DIR		Mr. Grau
R-TEST-DIR		Mr. Heimburg
R-TEST-C		Mr. Grafton
		Mr. Goetz
		Mr. Halbrooks
R-P&VE-DIR		Mr. Cline
		Mr. Hellebrand
		Mr. Palaoro
R-P&VE-A		Mr. Goerner
R-P&VE-V		Mr. Aberg
R-P&VE-S		Mr. Kroll
R-P&VE-M		Dr. Lucas
R-P&VE-P		Mr. Paul
		Mr. McCool
		Mr. Isbell
		Mr. Kuberg
R-P&VE-PE		Dr. Head
		Mr. Livingston
R-P&VE-PA		Mr. Thomson
R-P&VE-PM		Mr. Fuhrmann
R-P&VE-PP		Mr. Heusinger
R-P&VE-PT	(20)	Mr. Wood
		Mr. Stonemetz
R-P&VE-PR		Mr. Eby
R-P&VE-RT		Mr. Hofues
MS-IP		Mr. Remer
MS-IPL	(8)	Miss Robertson
MS-H		Mr. Akens
MS-T		

(25) Scientific and Technical Information Facility
Attn: NASA Representative (S-AK/RKT)
P. O. Box 5700
Bethesda, Maryland 20014

CC-P
I-RM-M